Integrated calibration of a 3D attitude sensor in large-scale metrology

Yang Gao[1], Jiarui Lin[1], Jigui Zhu[1], Jody Muelaner[2] and Patrick Keogh[2]

[1] State Key Laboratory of Precision Measuring Technology and Instruments, Tianjin University, Tianjin, 300072, China

[2] Department of Mechanical Engineering, University of Bath, Bath, BA2 7AY, UK

Abstract

A novel calibration method is presented for a sensor fusion system in large-scale metrology, which improves the calibration efficiency and reliability. The attitude sensor is composed of a pinhole prism, a converging lens, an area-array camera and a biaxial inclinometer. A mathematical model is established to determine its three-dimensional attitude relative to a cooperative total station by using two vector observations from the imaging system and the inclinometer. The measurement model developed has two aspects to be calibrated: the intrinsic parameters of the imaging model; and the transformation matrix between the camera and the inclinometer. An integrated calibration method using a three-axis rotary table and a total station is then proposed. A single mounting position of the attitude sensor on the rotary table is sufficient to solve for all parameters of the measurement model. A correction technique for the reference laser beam of the total station removes the need for accurate positioning of the sensor on the rotary table. Calibration measurements are made at multiple angular positions of the rotary table in order to determine all the unknown parameters in the model. Experimental verification has verified the practicality and accuracy of this calibration method. Results show that the mean deviations of attitude angles using the proposed method are less than 0.01°.

Keywords: sensor calibration; attitude measurement; large-scale metrology; large-volume metrology; sensor fusion system

1 Introduction

The problem of accurate attitude (orientation) measurement for rigid body objects is important in large-scale equipment manufacturing and the engineering of several domains including aircraft and spacecraft, ships, tunnel boring machines, and cranes [1-4]. Field measurement applications commonly require a sensor to have long range, high accuracy, be robust in harsh environments and be portable in use. For example, the underground guidance of tunnel boring machines requires measurement of real-time pose to within 10 mm and 1 mrad (about 0.057°) at a range of more than 100 m.

Several technologies and approaches are available to realize multi-dimensional

attitude measurement. One popular approach is based on using inertial sensors composed of multiple gyros and accelerometers [5]. The inertial based approach obtains positions and attitudes by calculating integrals of angular velocities and accelerations from the gyros and accelerometers, and is independent of external influences. However, its measurement errors tend to grow unbounded over time, and high-accuracy inertial units are very costly. Some sensor fusion techniques use aiding sensors, such as Global Navigation Satellite System (GNSS) or an electronic compass to help the inertial sensors mitigate the drift errors [6-8]. However, neither of them have a stable attitude accuracy better than 0.1°, besides, GNSS is not appropriate for use in indoor and underground environments, and electronic compasses may be influenced by local magnetic fields. Another existing method is to use optical or vision based observations of targets located on an object [9-11]. A typical method of determining the camera posture in computer vision is solving the so-called perspective-*n*-point (P*n*P) problems with multiple feature points. However, using a purely vision based method it is difficult to ensure good accuracy at more than 10 m of measurement range, and the fact that angular uncertainty increases with measurement range requires large target spaces for high accuracy and long range observations. 6-DOF probes based on laser trackers are commercially available. One such system, the Leica T-Mac uses a motorized camera on the tracker station to track the multiple points on the T-Mac probe [12]. It is a combination of laser tracking for position and P*n*P technique for orientation. Another such system, the API i360 probe combines a laser tracker with inclinometers and polarization of the laser to measure all the three attitude angles [13].

A number of patents describe a system in which a laser tracker is used to measure the position of a corner cube reflector with an aperture in the corner of the reflector. A portion of the beam passes onto a position detector located behind the aperture enabling pitch and yaw about the beam to be detected [REF's]. The final degree of freedom, roll about the beam, may be detected by, for example, imaging markers located around the reflector [REF] or by the polarization plane of the laser beam [REF].

Although the laser tracker based method has high accuracy, it also has limited measurement range, is extremely costly and is not suitable for engineering applications in harsh environments. Furthermore, many combined measurement scenarios using cameras, laser sensors, structured lights and mechanical devices have been proposed [14-16]. These are deficient in either range or accuracy.

Compared with the measurement systems described above, in large-scale metrology a total station instrument [17] is a popular tool in industrial and external engineering environments, offering advantages of flexibility in use, efficient measurement, long range (at least hundreds of meters), high accuracy (1-millimeter level), especially for angle measurement (1 arcsec level) and at reasonable cost ($2,000 to $20,000). However, a total station is a 3D coordinate measurement instrument, and it generally achieves 3D coordinate measuring by cooperation with an ordinary cube-

corner prism. The total station instrument cannot survey orientation directly which makes its applications limited. In this case, an attitude sensor for total station [18] (TS-attitude sensor) has been proposed. The TS-attitude sensor in [18] is composed mainly of a pinhole prism, a converging lens, an area-array camera and a biaxial inclinometer. By cooperating with this single sensor, which replaces the traditional prism, a total station can realize 3D attitude measurement with good accuracy. However, in [18], the calibration method for the attitude sensor uses two calibration setups in different steps, the whole process needs a large number of manual operations and adjustments, which may be unreliable, time-consuming and inefficient.

In the open literature on related calibration methods for attitude sensors for inertial systems [5] and star trackers [19], the multi-position tests are the common methods by mounting the sensor unit on a precise multi-axis rotary table. Motivated by the aforementioned studies, this paper proposes a novel calibration method for TS-attitude sensor in [18] which uses a three-axis rotary table and a total station as calibration tools to provide reference standard. After fixing a TS-attitude sensor on the three-axis rotary table just once, all the unknown parameters in the measurement model can be calibrated by different steps of multi-position tests.

The main contributions of this paper are as follows:

1) Establishment of a precise measurement model for TS-attitude sensor.

2) Proposal of a practical calibration method that enables different types of unknown parameters in the model to be calibrated in a single setup.

3) Presentation of a technique that makes the calibration simpler, without considering complex installation of the sensor in the calibration platform.

This paper is organized as follows. In Section 2, the configuration and the mathematical model of the attitude sensor are described. Section 3 introduces the integrated calibration method. Then, experimental validations are described in Section 4. Finally, concluding remarks and a brief overview of further work are presented.

2 Principle of Measurement

2.1 System Composition and Working Principle

The attitude measurement system this paper has two main units: a total station which acts as a base station; and a TS-attitude sensor which acts as a cooperative target. The function of the system is to determine the six degrees of freedom (including 3D position and 3D attitude) of the target sensor with respect to the stationary total station. The system prototype and composition are illustrated in Figure 1.

The TS-attitude sensor is very small and portable, being housed in an aluminum casing. The only exposed surface is the reflecting surface of the prism. The pinhole prism is adapted from a Leica standard circular prism whose vertex is cut in a small part to form a light channel. A converging lens and an area-array camera are designed behind the pinhole prism inside the sensor. The converging lens focuses at infinity and

its aperture diaphragm is at the pinhole of the prism. During measurement, the total station emits an approximately columnated measuring beam on the pinhole prism. Most of the light is reflected back by the prism which enables cooperative tracking as usual. The portion of light which passes through the pinhole is converged by the subsequent lens and finally produces a concentrated light spot on the imaging plane of the camera. The center of gravity method [20] is used to find a sub-pixel centroid of the spot. The location of the spot on the image plane gives the direction of the laser source and hence the orientation of the sensor in two degrees of freedom. The remaining degree of freedom, the rotation about the axis of the laser beam, is determined using a biaxial inclinometer located inside the sensor. Further, by the fusion of the detecting information from the imaging system and the inclinometer, the TS-attitude sensor finally obtains its 3D attitude in the coordinate system of the total station.

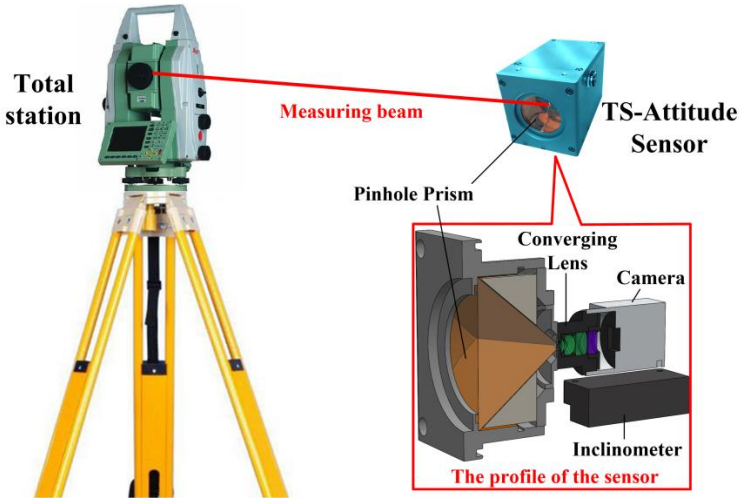

Figure 1. Prototype and composition of the attitude measurement system.

2.2 Measurement Model

The measurement model involves the following conventions:

- A single superscript to the left of a vector denotes its coordinate system, for example, a vector ${}^{T}\boldsymbol{v}$, is in frame *T*.
- The use of both a subscript and superscript denotes a transformation between two coordinate systems, for example, a rotation matrix ${}_{C}^{T}\boldsymbol{R}$ means its transformation is from frame *C* to frame *T*.
- A single subscript character following a matrix represents its state or sequence in a series of data. For example, a rotation matrix $\boldsymbol{R}_{(i)}$ means it is the *i*-th matrix in a series of matrixes (*i*=1, 2, …, *n*).

In the attitude measurement system, three different coordinate systems are defined: the total station frame ($O_TX_TY_TZ_T$-coordinate, frame *T*) as the reference coordinate system; the camera frame ($O_CX_CY_CZ_C$-coordinate, frame *C*); and the inclinometer frame ($O_IX_IY_IZ_I$-coordinate, frame *I*) in the sensor, as shown in Figure 2.

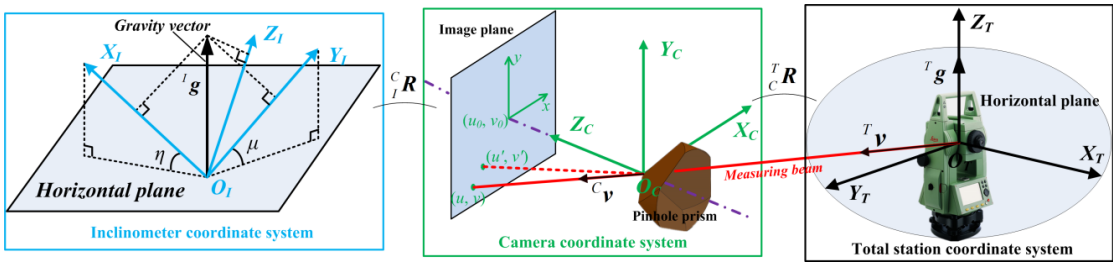

Figure 2. Definitions of all frames and their relationships in the attitude measurement.

A total station is a spherical coordinate measuring system, the origin O_T is the starting point of the ranging measurement. Therefore the unit vector of the measuring beam, ${}^{T}\boldsymbol{v}$ is obtained easily according to the measurement value of the total station. The Z_T-axis is perpendicular with the horizontal plane and therefore the gravity vector in frame T is ${}^{T}\boldsymbol{g} = [0 \quad 0 \quad 1]^{\mathrm{T}}$. Since frame T is a left-handed coordinate system (inherent in the definition of a total station), all the coordinate systems in this paper are defined as left-handed systems.

Unlike a traditional imaging system, which maps 3D points in the world coordinate system to 2D image points, the imaging system in the sensor instead maps the beam direction ${}^{T}\boldsymbol{v}$. Taking all the components in the light path including the prism into account, the reflection center of the prism where each incident rays intersect is the real optical center. Therefore, in frame C, the reflection center of the prism is defined as the origin O_C.

This imaging system conforms to the pinhole model with lens distortion. As shown in the camera frame definition part of Figure 3, the unit vector ${}^{C}\boldsymbol{v}$ denotes the vector of the laser beam in frame C, (u', v') denoting the real (distorted) image pixel coordinates, and (u, v) denoting ideal image pixel coordinates. According to the pinhole imaging model, the four-parameter model of a camera is given by

$$\begin{bmatrix} u \\ v \\ 1 \end{bmatrix} = \begin{bmatrix} a_x & 0 & u_0 \\ 0 & a_y & v_0 \\ 0 & 0 & 1 \end{bmatrix} \begin{bmatrix} {}^{C}v(x)/{}^{C}v(z) \\ {}^{C}v(y)/{}^{C}v(z) \\ 1 \end{bmatrix} = \begin{bmatrix} a_x & 0 & u_0 \\ 0 & a_y & v_0 \\ 0 & 0 & 1 \end{bmatrix} \begin{bmatrix} x \\ y \\ 1 \end{bmatrix} \tag{1}$$

where (u_0, v_0) denote the image coordinates of the camera's principal point, (x, y) are ideal normalized image coordinates, a_x and a_y are scale factors. Then, optical lens distortion is added to the ideal coordinates in order to obtain a precise model, and in this paper, only the first two terms of radial distortion are considered [21]. Let (x', y') be the real (distorted) normalized image coordinates. Now

$$\begin{cases} x' = x + x[k_1(x^2 + y^2) + k_2(x^2 + y^2)^2] \\ y' = y + y[k_1(x^2 + y^2) + k_2(x^2 + y^2)^2] \end{cases} \tag{2}$$

where k_1 and k_2 are the coefficients of the radial distortion. From $u' = u_0 + a_x x'$ and $v' = v_0 + a_y y'$, it follows that

$$\begin{cases} u' = u + (u - u_0)[k_1(x^2 + y^2) + k_2(x^2 + y^2)^2] \\ v' = v + (v - v_0)[k_1(x^2 + y^2) + k_2(x^2 + y^2)^2] \end{cases} \tag{3}$$

The imaging model has been established from laser beam vectors to the corresponding centroid of the spots. Also, as an inverse, the laser beam vector ${}^{C}\boldsymbol{v}$ can also be obtained from the corresponding centroid of the real spot (u', v') according to equation (3) ~ (1) with all the camera parameters calibrated.

The geometrical measurement model of a biaxial inclinometer is also shown in Figure 2. Observed data (η, μ) indicate the inclined angles between X_I-axis, Y_I-axis of the inclinometer and the horizontal plane. At this time, the unit vector of gravity direction in frame I is calculated by

$${}^{I}\boldsymbol{g} = \left[\sin\eta \quad \sin\mu \quad \sqrt{1 - \sin^2\eta - \sin^2\mu} \right]^{\mathrm{T}} \tag{4}$$

Now that the measurement model in each coordinate system has been described, the orientation transformation among them is defined. Suppose the attitude matrix from frame I to frame C is ${}^{C}_{I}\boldsymbol{R}$, and that from frame C to frame T is ${}^{T}_{C}\boldsymbol{R}$, which is the final goal. Since the gravity vector in frame C is obtained from that in frame I:

$${}^{C}\boldsymbol{g} = {}^{C}_{I}\boldsymbol{R} \cdot {}^{I}\boldsymbol{g} \tag{5}$$

then

$$\begin{cases} {}^{T}\boldsymbol{v} = {}^{T}_{C}\boldsymbol{R} \cdot {}^{C}\boldsymbol{v} \\ {}^{T}\boldsymbol{g} = {}^{T}_{C}\boldsymbol{R} \cdot {}^{C}\boldsymbol{g} \end{cases} \tag{6}$$

Thus, the calculation of the attitude between the total station and the sensor has become a problem of attitude determination using two vector observations: the laser beam vector and the gravity vector. According to Wahba's study [22], this problem is described as finding the proper orthogonal matrix ${}^{T}_{C}\boldsymbol{R}$ that minimizes the least-squares loss function

$$L({}^{T}_{C}\boldsymbol{R}) = \frac{1}{2}\left[p_1({}^{T}\boldsymbol{v} - {}^{T}_{C}\boldsymbol{R} \cdot {}^{C}\boldsymbol{v}) + p_2({}^{T}\boldsymbol{g} - {}^{T}_{C}\boldsymbol{R} \cdot {}^{C}\boldsymbol{g}) \right] \tag{7}$$

where p_1 and p_2 are weighting coefficients of each observation vectors. Their values are determined based on the angle measuring uncertainties of the imaging system and the inclinometer, respectively. This problem can be solved by the SVD (singular value decomposition) method that is presented by Markley in [23]. Define the matrix

$$\boldsymbol{B} = p_1 {}^{T}\boldsymbol{v} \, {}^{C}\boldsymbol{v}^{\mathbf{T}} + p_2 {}^{T}\boldsymbol{g} \, {}^{C}\boldsymbol{g}^{\mathbf{T}} \tag{8}$$

Then ${}^{T}_{C}\boldsymbol{R}$ is solved by the SVD method:

$${}^{T}_{C}\boldsymbol{R} = \boldsymbol{U}\left[1 \quad 1 \quad (\det\boldsymbol{U})(\det\boldsymbol{V}) \right]\boldsymbol{V}^{\mathbf{T}} \tag{9}$$

where $\boldsymbol{V}$ and $\boldsymbol{U}$ are right and left singular matrices of $\boldsymbol{B}$. The detailed derivation process

is explained in reference [23].

3 Integrated Calibration Method

3.1 Calibration Setups

In the measurement model of the system, there are two aspects should be calibrated in order to achieve measurement: the unknown intrinsic parameters $(a_x, a_y, u_0, v_0, k_1, k_2)$ of the imaging model, and the transformation matrix ${}^{C}_{I}\boldsymbol{R}$ between the coordinate systems of the camera and the inclinometer. Therefore, the calibration includes two steps and finally they are integrated together.

The calibration setup is shown in Figure 3(a). The three-axis rotary table used has four main components: the fixed base; the external frame which rotates around the horizontal-rotation axis with respect to the fixed base; the middle frame which rotates around the vertical-rotation axis with respect to the external frame; and the internal frame which rotates around the roll-rotation axis with respect to the middle frame. Notice that the rotary table used is levelled, which means that the horizontal-rotation axis is the same as the gravity direction. The TS-attitude sensor is mounted on the internal frame of the rotary table with the prism pointing towards the stationary total station, and the measurement laser beam of the total station is locked to the prism.

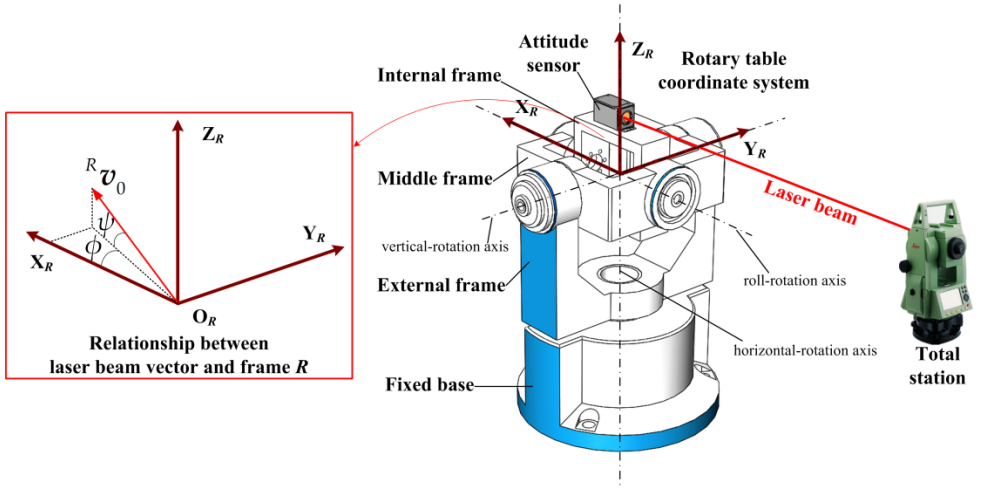

(**a**)

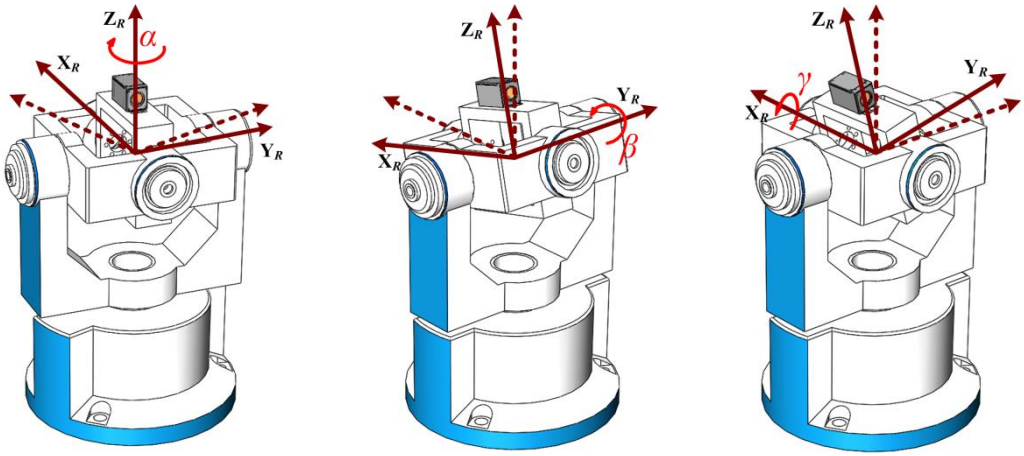

(**b**) (**c**) (**d**)

Figure 3. Calibration setup and rotation definition of the three-axis rotary table: (**a**) Calibration setup description; (**b**) Horizontal rotation of the rotary table; (**c**) Vertical rotation of the rotary table; (**d**) Roll rotation of the rotary table.

A rotary table coordinate frame ($O_RX_RY_RZ_R$-coordinate, frame R) is defined on the internal frame, its origin is on the rotary center, and in the default position, the Z_R-axis, Y_R-axis and X_R-axis are the same as the horizontal-rotation, vertical-rotation and roll-rotation axes. At this position, the default rotation is at horizontal angle $\alpha = 0°$, vertical angle $\beta = 0°$, and roll angle $\gamma = 0°$. The rotating sketch of all the three axes are plotted in Figures 3(b), (c), and (d).

In a situation where the internal frame and the sensor is rotated by horizontal angle $\alpha_{(i)}$ ($i = 0, 1, 2, \ldots, l$), vertical angle $\beta_{(j)}$ ($j = 0, 1, 2, \ldots, m$) and roll angle $\gamma_{(k)}$ ($k = 0, 2, \ldots, n$), the relative attitude of frame R with respect to the fixed base has changed, and this attitude transformation can be expressed by the rotation matrix

$$ {}^{R}\boldsymbol{R}_{(i,j,k)} = \begin{bmatrix} 1 & 0 & 0 \\ 0 & \cos\gamma_{(k)} & \sin\gamma_{(k)} \\ 0 & -\sin\gamma_{(k)} & \cos\gamma_{(k)} \end{bmatrix} \begin{bmatrix} \cos\beta_{(j)} & 0 & -\sin\beta_{(j)} \\ 0 & 1 & 0 \\ \sin\beta_{(j)} & 0 & \cos\beta_{(j)} \end{bmatrix} \begin{bmatrix} \cos\alpha_{(i)} & \sin\alpha_{(i)} & 0 \\ -\sin\alpha_{(i)} & \cos\alpha_{(i)} & 0 \\ 0 & 0 & 1 \end{bmatrix} \tag{10} $$

Note that by definition, $\alpha_{(0)} = 0°$, $\beta_{(0)} = 0°$ and $\gamma_{(0)} = 0°$. The specific calibration process is described in the following subsections.

3.2 Calibration of the Imaging Model

An external frame rotates around the horizontal-rotation axis of the rotary table, and the middle frame rotates around the vertical-rotation axis to calibrate the imaging model. By changing multiple angular positions of these two frames, for the sensor on the rotary table in front of the reference laser beam from the total station an accurate control field of the laser beam can be constructed.

The reflection center of the prism should be adjusted relative to the rotary center of the rotary table in order to make sure that during rotation, the laser beam vector from the total station to the prism remains stationary. However, in order to avoid the rotary table blocking the light path, the TS-attitude sensor has to be mounted offset from the rotary center and above the X_RY_R -plane. As a result, the reflection center of the sensor varies in both vertical and horizontal directions relative to the fixed base during the rotating around all the axes, as shown in Figure 4.

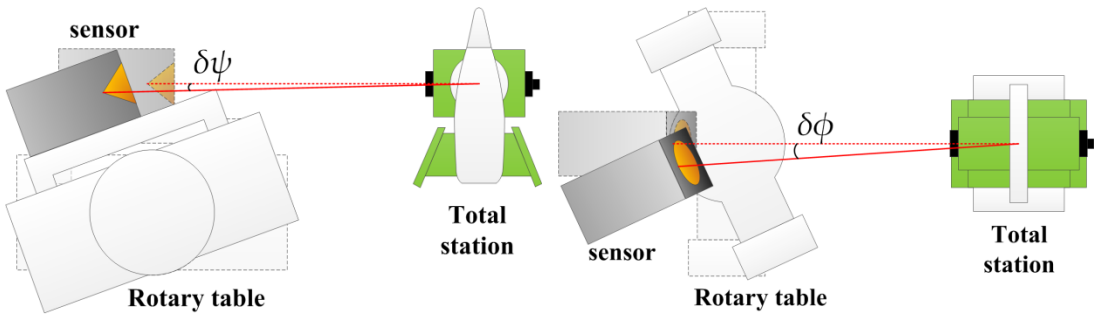

(**a**) (**b**)

Figure 4. Relationship between the laser beam and the sensor in the calibration process: (**a**) Angle deviation in vertical direction; (**b**) Angle deviation in horizontal direction.

Since the sensor is tracked by the total station continuously in the lock mode, by reading the deviation values of the horizontal and vertical angles from the total station, the reference laser beam can be corrected. Actually, because of the utilization of the total station, the demand of the sensor installation on the rotary table is not essential. In the setup of the calibration, the height of the total station is adjusted to ensure that the measurement beam is leveled in the default position of the rotary table. In this situation, the laser beam vector in frame *R* can be expressed as follows:

$$ {}^{R}\boldsymbol{v}_0 = \begin{bmatrix} \cos(\varphi + \delta\varphi)\cos(\psi + \delta\psi) \\ \sin(\varphi + \delta\varphi)\cos(\psi + \delta\psi) \\ \sin(\psi + \delta\psi) \end{bmatrix} \tag{11} $$

where (φ, ψ) are yaw and pitch angles, respectively, which are illustrated in Figure 4(a), and ($\delta\varphi$, $\delta\psi$) are the corresponding deviation angles. The value of φ is unknown, and since the rotary table and total station are both levelled, $\psi = 0°$. The values of ($\delta\varphi$, $\delta\psi$) are directly obtained by the total station as illustrated in Figure 4.

During the camera calibration, no motion around the roll-rotation axis is maintained. In a position where the internal frame and the sensor are rotated by the horizontal angle $\alpha_{(i)}$ (*i*-th position) and vertical angle $\beta_{(j)}$ (*j*-th position), the relative attitude of frame *R* with respect to the fixed base or its default position has changed, and the laser beam vector in frame *R* has been transformed as

$$ {}^{R}\boldsymbol{v}_{(i,j)} = {}^{R}\boldsymbol{R}_{(i,j,0)} \cdot {}^{R}\boldsymbol{v}_0 \tag{12} $$

where the definition of ${}^{R}\boldsymbol{R}_{(i,j,0)}$ is the same as equation (10).

Suppose the rotation matrix from frame *R* to frame *C* is ${}^{T}_{C}\boldsymbol{R}$, then the laser beam vector in frame *C* is expressed as

$$ {}^{C}\boldsymbol{v}_{(i,j)} = {}^{C}_{R}\boldsymbol{R} \cdot {}^{R}\boldsymbol{v}_{(i,j)} = {}^{C}_{R}\boldsymbol{R} \cdot {}^{R}\boldsymbol{R}_{(i,j,0)} \cdot \begin{bmatrix} \cos(\varphi + \delta\varphi)\cos(\delta\psi) \\ \sin(\varphi + \delta\varphi)\cos(\delta\psi) \\ \sin(\delta\psi) \end{bmatrix} \tag{13} $$

Equation (13) establishes the exact relationship between the laser beam vector and the camera coordinate system via the two-dimensional rotary transformation of the rotary table. Equation (13) represents an extrinsic parameter model in which the parameters. Further, suppose $(u'_{(i,j)}, v'_{(i,j)})$ in the image plane is the projection of beam vector ${}^{C}\boldsymbol{v}_{(i,j)}$ according to equations (3) ~ (1) of the intrinsic parameter model in Section 2.2, then the whole measurement model of the imaging system is established.

For $l \times m$ different rotation positions of the rotary table during calibration, the image position of detected laser spot is given by $(\hat{u}_{(i,j)}, \hat{v}_{(i,j)})$ where the external frame is in *i*-th position and the middle frame is in *j*-th position. All the unknowns

$(\varphi, {}^{C}_{R}\boldsymbol{R}, a_x, a_y, u_0, v_0, k_1, k_2)$ in this model can be obtained by minimizing the following function:

$$J(\varphi, {}^{C}_{R}\boldsymbol{R}, a_x, a_y, u_0, v_0, k_1, k_2) = \sum_{j=1}^{m}\sum_{i=1}^{l}[(\hat{u}_{(i,j)} - u'_{(i,j)})^2 + (\hat{v}_{(i,j)} - v'_{(i,j)})^2] \tag{14}$$

This nonlinear minimization problem can be solved using optimization techniques such as the Levenberg–Marquardt algorithm [24]. Note that reasonable initial values should be given for a global optimal solution.

3.3 Calibration Between the Inclinometer and the Rotary Table

Since the rotation matrix between coordinate systems of the camera and rotary table has been calibrated, by calibrating the transformation between the inclinometer and the rotary table, the final rotation ${}^{C}_{I}\boldsymbol{R}$ can be obtained. A practical and high-precision method is presented by changing multiple angular positions of the rotary table's middle frame and internal frame. Because the rotary table is levelled, in the default position the unit vector of the gravity direction in frame R is ${}^{T}\boldsymbol{g} = [0 \quad 0 \quad 1]^{\mathrm{T}}$.

During calibration, no motion is maintained around the horizontal-rotation axis and in a position where the internal frame and the sensor are rotated by vertical angle $\beta_{(j)}$ (j-th position) and roll angle $\gamma_{(k)}$ (k-th position). The relative attitude of frame R with respect to the fixed base or its default position changes, hence the gravity vector in frame R is transformed as

$${}^{R}\boldsymbol{g}_{(j,k)} = {}^{R}\boldsymbol{R}_{(0,j,k)} \cdot {}^{R}\boldsymbol{g}_0 \tag{15}$$

where the definition of ${}^{R}\boldsymbol{R}_{(0,j,k)}$ is the same as equation (10). Substituting for ${}^{R}\boldsymbol{R}_{(0,j,k)}$ by (10) in (15), simplifying and results in

$${}^{R}\boldsymbol{g}_{(j,k)} = \begin{bmatrix} 1 & 0 & 0 \\ 0 & \cos\gamma_{(k)} & \sin\gamma_{(k)} \\ 0 & -\sin\gamma_{(k)} & \cos\gamma_{(k)} \end{bmatrix} \begin{bmatrix} \cos\beta_{(j)} & 0 & -\sin\beta_{(j)} \\ 0 & 1 & 0 \\ \sin\beta_{(j)} & 0 & \cos\beta_{(j)} \end{bmatrix} \begin{bmatrix} 0 \\ 0 \\ 1 \end{bmatrix} = \begin{bmatrix} -\sin\beta_{(j)} \\ \sin\gamma_{(k)}\cos\beta_{(j)} \\ \cos\gamma_{(k)}\cos\beta_{(j)} \end{bmatrix} \tag{16}$$

Since the rotation matrix from frame R to frame I is ${}^{I}_{R}\boldsymbol{R}$, the gravity vector in frame I can be calculated from that in frame R as

$${}^{I}\boldsymbol{g}_{(j,k)} = {}^{I}_{R}\boldsymbol{R} \cdot {}^{R}\boldsymbol{g}_{(j,k)} = {}^{I}_{R}\boldsymbol{R} \cdot \begin{bmatrix} -\sin\beta_{(j)} \\ \sin\gamma_{(k)}\cos\beta_{(j)} \\ \cos\gamma_{(k)}\cos\beta_{(j)} \end{bmatrix} \tag{17}$$

Since the gravity vector in frame I is measured directly according to equation (4), substituting for ${}^{I}\boldsymbol{g}_{(j,k)}$ from (4), equation (17) is transformed as

$$ {}^{I}_{R}\boldsymbol{R}\cdot\begin{bmatrix} -\sin\beta_{(j)} \\ \sin\gamma_{(k)}\cos\beta_{(j)} \\ \cos\gamma_{(k)}\cos\beta_{(j)} \end{bmatrix} = \begin{bmatrix} \sin\eta_{(j,k)} \\ \sin\mu_{(j,k)} \\ \sqrt{1-\sin^2\eta_{(j,k)}-\sin^2\mu_{(j,k)}} \end{bmatrix} \tag{18} $$

where the observed $(\eta_{(j,k)}, \mu_{(j,k)})$ indicate the inclined angles from the inclinometer in a position of the rotary table where the vertical-rotation angle is $\beta_{(j)}$ and roll-rotation angle is $\gamma_{(k)}$. By stacking $m \times n$ such equations as (18) together,

$$ {}^{I}_{R}\boldsymbol{R}\cdot\begin{bmatrix} -\sin\beta_{(1)} & \cdots & -\sin\beta_{(m)} \\ \sin\gamma_{(1)}\cos\beta_{(1)} & \cdots & \sin\gamma_{(n)}\cos\beta_{(m)} \\ \cos\gamma_{(1)}\cos\beta_{(1)} & & \cos\gamma_{(n)}\cos\beta_{(m)} \end{bmatrix} = \begin{bmatrix} \sin\eta_{(1,1)} & \cdots & \sin\eta_{(m,n)} \\ \sin\mu_{(1,1)} & \cdots & \sin\mu_{(m,n)} \\ \sqrt{1-\sin^2\eta_{(1,1)}-\sin^2\mu_{(1,1)}} & & \sqrt{1-\sin^2\eta_{(m,n)}-\sin^2\mu_{(m,n)}} \end{bmatrix} \tag{19} $$

Equation (19) can be simplified to a matrix equation in form of ${}^{I}_{R}\boldsymbol{R}\boldsymbol{A} = \boldsymbol{D}$, and ${}^{I}_{R}\boldsymbol{R}$ may be solved by in terms of the SVD:

$$ {}^{I}_{R}\boldsymbol{R} = \boldsymbol{V}\boldsymbol{U}^{\mathrm{T}} \tag{20} $$

where $\boldsymbol{V}$ and $\boldsymbol{U}$ are right and left singular matrices of $\boldsymbol{A}\boldsymbol{D}^{\mathrm{T}}$.

3.4 Calibration Summary

According to the result of Subsections 3.2 and 3.3, the final rotation between the coordinate systems of the inclinometer and the camera is obtained as

$$ {}^{C}_{I}\boldsymbol{R} = {}^{C}_{R}\boldsymbol{R}\cdot{}^{I}_{R}\boldsymbol{R}^{\mathrm{T}} \tag{21} $$

and to summarize, the basic block diagram of the whole calibration process is shown in Figure 5.

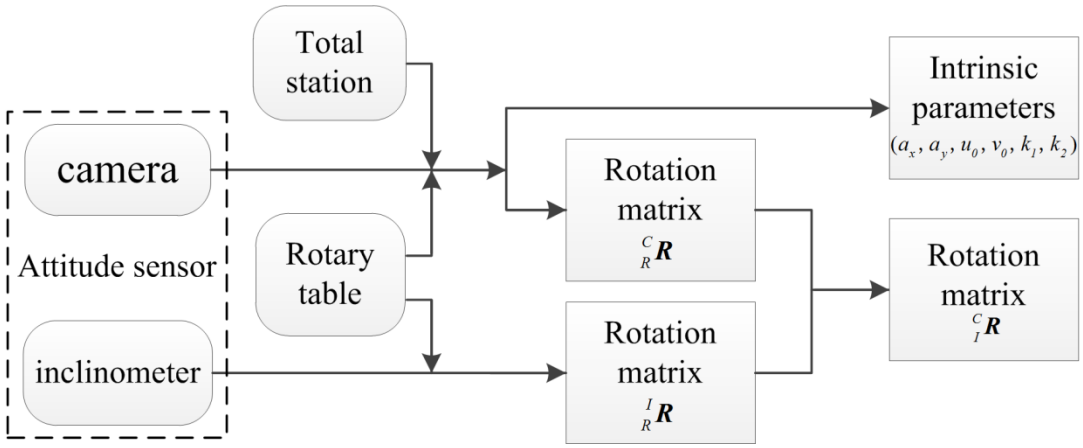

Figure 5. Block diagram of calibration implementation.

4 Experiments

The camera used in the TS-attitude sensor had 1280 × 1024 pixels each of 5.3 μm × 5.3 μm in size. The converging lens designed had a 12 mm focal length, which determines the field of view to be approximately 33° × 27°. The inclinometer in the sensor had a measurement range of ±15° in both axes, and its measurement maximum

permissible error (MPE) was 0.005°. After the camera and the inclinometer were installed in the sensor, X_I-axis was nearly parallel to the Z_C-axis, and Y_I-axis was nearly parallel to the X_C-axis due to the precision of the machining. The three-axis rotary table used had an angle measurement accuracy of 1 arcsec. A Leica TS15 total station with angle measurement uncertainty of 1 arcsec was used for these experiments. The calibration platform is shown in Figure 6.

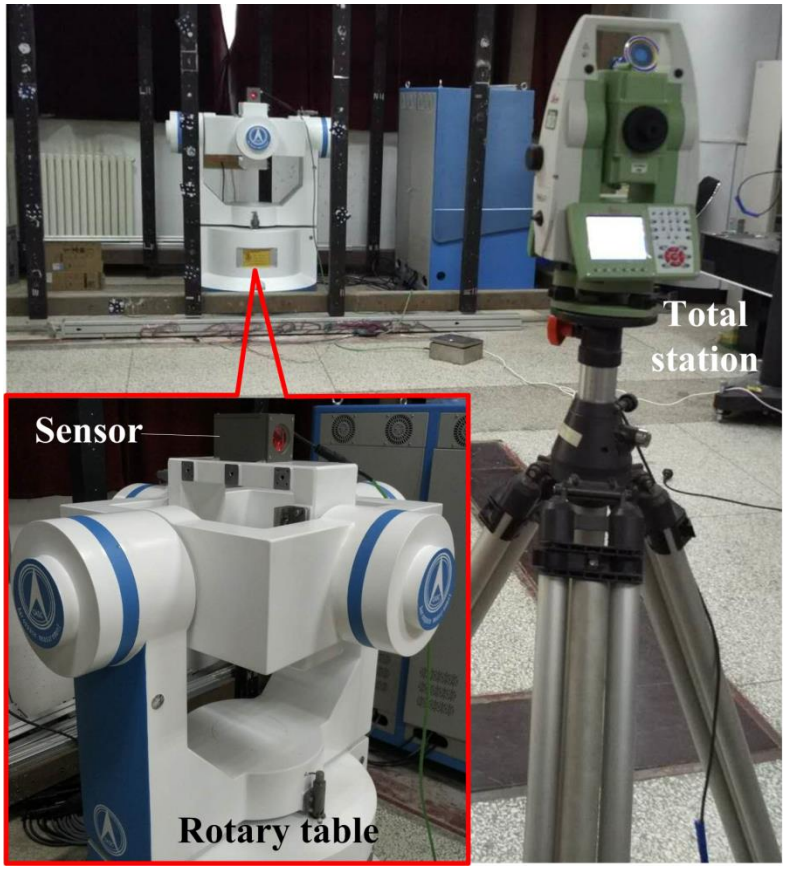

Figure 6. Experimental and verification platform for the proposed method.

In the ideal case, the values of the intrinsic parameters of the imaging model are as listed in Table 1: the scale factor is the quotient of the designed focal length divided by the pixel size, the principal point values are the half of the pixel numbers, and all distortion coefficients are set to zero. The value of rotation matrix ${}^{C}_{I}\boldsymbol{R}$ in the ideal situation is also listed in Table 1, which was calculated according to the installation relationship between the camera and the inclinometer.

Table 1. Ideal values and calibrated results of the unknown parameters in the model.

	a_x	a_y	u_0	v_0	k_1	k_2	${}^{C}_{I}\boldsymbol{R}$
Ideal value	2264.15	2264.15	640	512	0	0	$\begin{bmatrix} 0 & 1 & 0 \\ 0 & 0 & 1 \\ 1 & 0 & 0 \end{bmatrix}$

Calibrated result	2269.28	2269.53	628.28	509.80	0.045	-0.007	$\begin{bmatrix} -0.0135 & 0.9999 & 0.0053 \\ 0.0036 & -0.0052 & 0.9999 \\ 0.9999 & 0.0135 & -0.0035 \end{bmatrix}$

During the calibration of imaging model, the horizontal-rotation axis was rotated from -15° to 15°, and vertical-rotation axis from -12° to 12°, respectively, both with a 2° step, which results in 16 × 13 = 208 groups of calibration data. During the calibration for ${}^{I}_{R}\boldsymbol{R}$, the vertical-rotation axis and roll-rotation axis were both rotated from -10° to 10° with a 5° step, which results in 5 × 5 = 25 groups of calibration data. By control of an automated program, the whole calibration process was completed in less than 30 minutes without human intervention.

The calibration results are also listed in Table 1, and they are evidently different with the ideal values. In addition, the RMS residual distance error of the laser spot center is 0.23 pixel, which corresponds to equivalent RMS angle error of 0.0059° according to the imaging model. Also, the RMS residual error of the inclinometer calibration is 0.0025°. These results verify the feasibility and effectiveness of the calibration approach.

The final performance of the TS-attitude sensor was also evaluated using the rotary table as an angle standard. In order for a direct comparison, the attitude matrix of the sensor was parameterized by three Euler angles: yaw, pitch, and roll, corresponding to the horizontal-rotation, vertical-rotation and roll-rotation angles of the rotary table. The attitude measurement system was inspected at 27 different random positions of the rotary table with the proposed method, and measurement values were compared with the ground reference obtained directly from the rotary table. In addition, the experiment data were also processed by the model with uncalibrated parameters which were set by ideal values. The results of the 3D angle deviation are plotted in Figure 7, showing that by using the proposed method the mean deviation of these 27 sets of result is (0.0066°, 0.0018°, 0.0023°). As a comparison, Figure 8 shows the mean deviation processed by the model without calibration as (0.0193°, 0.0119°, 0.0163°). Figure 7 shows that the variability in the yaw angle measurement is larger than that of pitch and roll angles, this is because the yaw angle is almost completely determined by the imaging system whose measurement accuracy is lower than that of the inclinometer. This phenomenon is not clear in Figure 8 because the effect of uncalibrated parameters is much larger than the random effects in the measuring units.

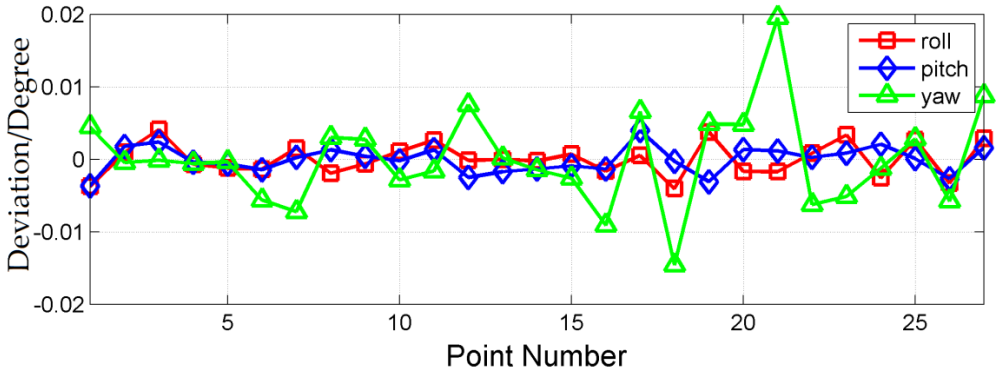

Figure 7. The 3D angle deviations in verification experiment using proposed method.

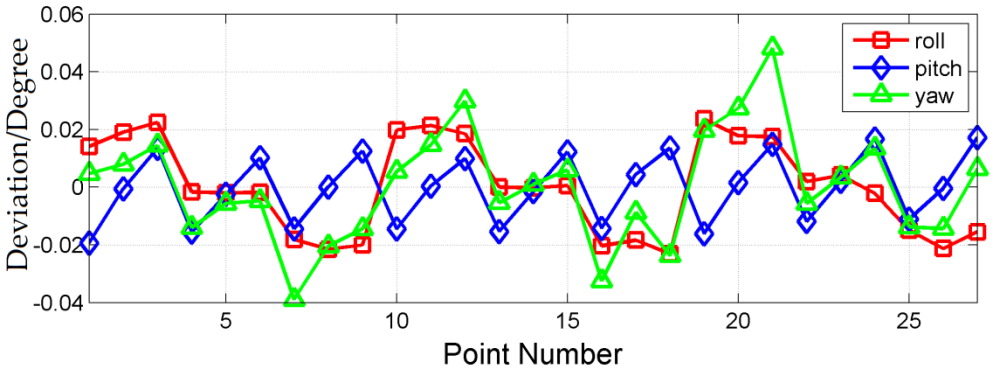

Figure 8. The 3D angle deviations in verification experiment using uncalibrated parameters.

5 Conclusions

This paper has proposed a novel calibration method for an accurate 3D attitude sensor to improve the calibration efficiency and reliability. The configuration and measurement principle of the sensor have been introduced, and a mathematical model has also been developed to obtain the 3D attitude of the sensor with respect to the cooperative total station. The new calibration method enables all the unknown parameters in the measurement model (the intrinsic parameters of the imaging model. It also enables the transformation matrix between the camera and the inclinometer) to be calibrated with a single placement on the three-axis rotary table without considering accurate location of the installed sensor. Therefore, the method is very significant for engineering applications.

In the practical experiment, by the control of an automated program, the whole calibration process has been completed in less than 30 minutes without human intervention. For validation, the performance of the calibrated sensor system has compared with that without calibration. The evaluation experiments have shown that the mean deviation of yaw, pitch, and roll angles using the proposed method are (0.0066°, 0.0018°, 0.0023°) compared with (0.0193°, 0.0119°, 0.0163°) using uncalibrated parameters.

The calibration method described here could be applied in other attitude measurement systems based on sensor fusion. Future work may benefit greatly by

studying more complicated camera model.

Acknowledgments

This work was funded by the National Natural Science Foundation of China (Grant No. 51405338, 51305297, 51225505) and the Natural Science Foundation of Tianjin (Grant No. 15JCQNJC04600). The support of the EPSRC through the Light Controlled Factory project, EP/K018124/1, is also acknowledged.

References

[1] C. K. Rao, P. Mathur, S. Pathak, S. Sundaram, R. R. Badagandi, and K. V. Govinda, A novel approach of correlating optical axes of spacecraft to the RF axis of test facility using close range photogrammetry. *Journal of Optics*, vol. 42, pp. 51-63, 2013.

[2] X. S. Shen, M. Lu, and W. Chen, Tunnel-Boring Machine Positioning during Microtunneling Operations through Integrating Automated Data Collection with Real-Time Computing. *Journal of Construction Engineering and Management-Asce*, vol. 137, pp. 72-85, Jan 2011.

[3] Marjetič A, Kregar K, Ambrožič T, et al. An alternative approach to control measurements of crane rails. *Sensors*, 2012, 12(5): 5906-5918.

[4] Y. K. Kim, Y. Kim, S. J. Yun, I. G. Jang, K. S. Kim, S. Kim, et al. Developing Accurate Long-Distance 6-DOF Motion Detection With One-Dimensional Laser Sensors: Three-Beam Detection System. *IEEE Transactions on Industrial Electronics*, vol. 60, pp. 3386 - 3395, 2013.

[5] Titterton, D.H.; Weston, J.L. *Strapdown Inertial Navigation Technology*; Peter Peregrinis: London, UK, 1997.

[6] Metge, J., et al. Calibration of an inertial-magnetic measurement unit without external equipment, in the presence of dynamic magnetic disturbances. *Measurement Science and Technology* 25.12 (2014): 125106.

[7] Ren Y, Wang Y, Wang M, et al. A Measuring System for Well Logging Attitude and a Method of Sensor Calibration. *Sensors*, 2014, 14(5): 9256-9270.

[8] Yang, Yingdong, Xuchu Mao, and Weifeng Tian. A novel method for low-cost MIMU aiding GNSS attitude determination. *Measurement Science and Technology* 27.7 (2016): 75003-75013.

[9] Skaloud J, Cramer M, Schwarz K P. Exterior orientation by direct measurement of camera position and attitude. *International Archives of Photogrammetry and Remote Sensing*, 1996, 31(B3): 125-130.

[10] T. Luhmann, Precision potential of photogrammetric 6DOF pose estimation with a single camera. *ISPRS Journal of Photogrammetry and Remote Sensing*, vol. 64, pp. 275-284, May 2009.

[11] Y. Zheng, Y. Kuang, S. Sugimoto, et al. Revisiting the PnP Problem: A Fast, General and Optimal Solution, *2013 IEEE International Conference on Computer Vision (ICCV)*, 2013, pp. 2344-2351.

[12] Böckem, Burkhard. Laser tracker with a target sensing unit for target tracking and orientation detection, US9322654. 2016.
[13] Lau, Kam C. Accurate target orientation measuring system. US, US7400416. 2008.
[14] Y. H. Li, Y. R. Qiu, Y. X. Chen, et al. A novel orientation and position measuring system for large & medium scale precision assembly. *Optics and Lasers in Engineering*, vol. 62, pp. 31-37, Nov 2014.
[15] Myung H, Lee S, Lee B. Paired Structured Light for Structural Health Monitoring Robot System. *Structural Health Monitoring*, 2010, 9(3):49-64.
[16] Kim, Young-Keun, et al. Design improvement of the three-beam detector towards a precise long-range 6-degree of freedom motion sensor system. *Review of Scientific Instruments* 85.1 (2014): 015004.
[17] Schmitt, R. H., et al. "Advances in Large-Scale Metrology–Review and future trends." *CIRP Annals-Manufacturing Technology* 65.2 (2016): 643-665.
[18] Yang Gao, Jiarui Lin, Linghui Yang, et al. Development and calibration of an accurate 6-degree-of-freedom measurement system with total station. *Measurement Science and Technology* 27.12 (2016): 125103.
[19] Wei X, Zhang G, Fan Q, et al. Star sensor calibration based on integrated modelling with intrinsic and extrinsic parameters. Measurement, 2014, 55: 117-125.
[20] G. Rufino and D. Accardo, Enhancement of the centroiding algorithm for star tracker measure refinement. *Acta Astronautica*, vol. 53, pp. 135-147, Jul 2003.
[21] Z. Zhang, A Flexible New Technique for Camera Calibration. *IEEE Transactions on Pattern Analysis and Machine Intelligence*, 1998, pp. 1330--1334.
[22] Wahba, GRACE. A least squares estimate of spacecraft attitude. SIAM Review , 1965 , 7(3): 409.
[23] Markley F L. Attitude determination using vector observations and the singular value decomposition. The Journal of the Astronautical Sciences, 1988, 36(3): 245-258.
[24] Moré J J. The Levenberg-Marquardt algorithm: Implementation and theory. *Lecture Notes in Mathematics*, 1978, 630:105-116.